

# DEOXYTHYMIDINE SUGARS ARE NOT DIRECT PRECURSORS OF DNA-THYMINE

JAMES LOEHR AND PHILIP HANAWALT, *Department of Biological Sciences,  
Stanford University, Stanford, California 94305 U.S.A.*

**ABSTRACT** A theoretical model for the kinetics of uptake of a putative precursor molecule into nucleotide pools and into replicating DNA has been developed. The relationship between the accumulation of radioactively labeled precursors in the pool and the appearance of radioactivity in DNA is then derived. Experiments have been carried out in bacteria to compare the uptake of radioactive thymine into deoxythymidine triphosphate, deoxythymidine diphosphate sugars, and DNA to test the suitability of either compound as the direct precursor of thymine in DNA. New one-dimensional, thin-layer chromatographic procedures were used to determine the specific activity of deoxythymidine triphosphate and deoxythymidine diphosphate sugars in growing cultures of  $^{32}\text{PO}_4$ -labeled *Escherichia coli* during pulse labeling with [ $^3\text{H}$ ]-thymine. A comparison of the experimental data with our theoretical model supports the hypothesis that deoxythymidine triphosphate, but not deoxythymidine sugar, is the direct precursor of thymine in normally replicating DNA *in vivo*.

## INTRODUCTION

Deoxynucleoside triphosphates (dNTPs) have been employed as substrates for the *in vitro* synthesis of DNA by purified DNA polymerases. This polymerization reaction is accompanied by the release of the  $\beta$  and  $\gamma$  phosphates of the precursors as inorganic pyrophosphate and the subsequent hydrolysis of the pyrophosphate by inorganic pyrophosphatase (Kornberg, 1974); thus, all three phosphate moieties on the precursor nucleotide are essential for *in vitro* DNA replication. Deoxynucleoside triphosphates also support polymerase-directed DNA synthesis in toluene-permeabilized bacteria (Moses and Richardson, 1970; Masker and Hanawalt, 1973) and spermidine-stabilized *E. coli* chromosomes *in vitro* (Kornberg et al., 1974; Kornberg, 1975).

The only DNA polymerase known to be required for bacterial DNA replication both *in vivo* and *in vitro* is DNA polymerase III, coded for by the *dna E* locus (Gefter et al., 1971; Nüsslein et al., 1971). It is important to note that several of the properties ascribed to DNA polymerases (such as single binding site for all deoxynucleoside triphosphates and the importance of the triphosphate moiety for substrate binding to the enzyme) have been shown to be true only for DNA polymerase I and have not yet been investigated for DNA polymerase III. Of particular interest is the fact that DNA polymerase III has a lower affinity for triphosphates than do either polymerase I or II (Kornberg, 1974); the reaction conditions used for polymerase III may have been suboptimal for triphosphate binding, or perhaps the actual *in vivo* precursor is a different molecule.

The only *in vivo* studies reported on the suitability of deoxynucleoside triphosphates as

---

Dr. Loehr's present address is Washington University Medical School, St. Louis, Mo. 63110.

DNA synthesis precursors are those of Werner (1971), in which an attempt was made to relate the kinetics of infiltration of [ $^3\text{H}$ ]-thymine into intracellular deoxythymidine monophosphate (dTMP), deoxythymidine diphosphate (dTDP), and deoxythymidine triphosphate (dTTP), and DNA. An analysis of his data by Rubinow and Yen (1972) indicated that dTDP was the most suitable of the three nucleotides as DNA precursors. Unfortunately, their analysis was complicated in at least two important ways: (a) Although they assumed that there was a steady flux of thymine through the intracellular nucleotide pools and into DNA, it is not certain that the cultures used by Werner (concentrated to a density of  $2 \times 10^{10}/\text{ml}$  at  $14^\circ\text{C}$ ) were actually in balanced growth at the time the experiment was performed; and (b) only three points from Werner's DNA synthesis data could be used in curve fitting to the theoretically predicted values. In a linear regression such as that performed by Rubinow and Yen an estimate of the error variance is directly proportional to the factor  $(1/[N-2])$ , where  $N$  is the number of data points (Goldstein, 1964). The error variance of a linear regression drawn from 3 points is therefore 10 times that of a regression from 12 points. No error estimate was made by Rubinow and Yen.

Two independent groups of investigators have reported the existence of a large intracellular dTDP sugar (dTDP-sugar) pool in *E. coli* (Hosono et al., 1975; Ohkawa, 1976); depending upon the bacterial strain and growth conditions used, the dTDP-sugar pool may be seven times as large as the dTTP pool. Several dTDP-sugars had previously been isolated, but their metabolic fates are not well known. TDP-L-rhamnose, which can be formed enzymatically from dTDP-D-glucose (Okazaki et al., 1960; Okazaki et al., 1963), is a major carrier of rhamnose to the cell wall, where rhamnose may be involved in bacteriophage P4 adsorption (Kahn, 1976). dTDP-sugars were not included in Werner's investigations.

We have performed an experiment relating the uptake of radioactive thymine into dTTP, dTDP-sugars and DNA to test the suitability of either nucleotide pool as the direct precursor pool for thymine in DNA. Exponentially growing thymine-requiring *E. coli* K12 were diluted slightly into fresh preconditioned medium containing radioactive thymine, and the change of the specific activity of the pools in time and the accumulation of radioactive material into DNA were followed. A comparison of these experimental data with our theoretical model supports the hypothesis that dTTP, and not dTDP-sugar, is the direct precursor of thymine in DNA *in vivo*.

## THEORETICAL

### *Kinetics of Uptake of Radioactivity into Acid-Soluble Nucleotide Pools*

A bacterial population in a steady state of balanced exponential growth can be expressed by the relation

$$N_t = N_0 e^{\nu t} \quad (1)$$

where  $N_0$  and  $N_t$  represent the number of cells at time 0 and time  $t$ , respectively, and  $\nu$  is the growth constant defined by the equation

$$\nu \tau = \ln 2, \quad (2)$$

where  $\tau$  is the time required for the population to double in size (Powell, 1956). The number of

precursor pools,  $P_t$ , and the number of DNA replication forks,  $Q_t$ , can be expected to increase in a similar manner, that is:

$$P_t = P_0 e^{rt}, \quad (3)$$

and

$$Q_t = Q_0 e^{rt}. \quad (4)$$

When either  $N_t$ ,  $P_t$ , or  $Q_t$  are plotted against time,  $t$ , the result is an exponential curve; if plotted vs. relative cell mass (which increases exponentially with time) the plot is a straight line with a slope of unity.

If the size of any individual intracellular pool remains constant over time (which, when averaged over the entire population, will be true if the culture is in balanced growth), then the rate at which molecules enter the pool ( $\alpha$ ) and leave the pool ( $\beta$ ) must be identical. If the size of the pool is symbolized by  $m$ , the number of nonradioactive molecules in the pool defined as  $U_t$ , and the number of radioactive molecules in the pool described as  $L_t$ , the situation can be visualized in this fashion (Cooper, 1973):

$$\alpha \{L_t + U_t\} \beta.$$

There are no radioactive molecules in the pool at time = 0; therefore,

$$L_0 = 0 \text{ and } U_0 = m.$$

The rate of uptake of labeled molecules into the pool is given by

$$\frac{dL}{dt} = \alpha - \beta(L_t/m) = \alpha - \beta(L_t/[L_t + U_t]). \quad (5)$$

If the population is unable to synthesize those molecules *de novo*, but must instead acquire them from the medium (which is true for the thymine-requiring strain used in our experiments), and if this raw material (thymine) has a specific activity,  $A$  (in, for example,

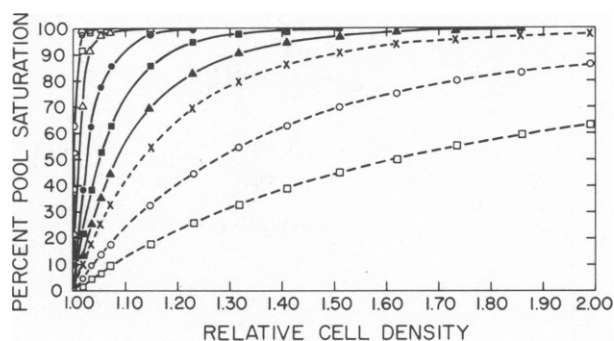


FIGURE 1 Theoretical change in the specific activity of an intracellular acid-soluble pool with increasing cell density according to the equation  $p(t) = 1 - e^{-at/m}$ . The doubling time used is 201.33 min. The different values for  $\alpha/m$  shown are: 1.00,  $\circ-\circ$ ; 0.75,  $\circ-\circ$ ; 0.50,  $\square-\square$ ; 0.25,  $\Delta-\Delta$ ; 0.10,  $\bullet-\bullet$ ; 0.05,  $\blacksquare-\blacksquare$ ; 0.03,  $\blacktriangle-\blacktriangle$ ; 0.02,  $\times-\times$ ; 0.01,  $\bigcirc-\bigcirc$ ; 0.005,  $\square-\square$ .

disintegrations  $\text{min}^{-1} \text{mol}^{-1}$ ), then the solution to Eq. 5 becomes:

$$p(t) = A(1 - e^{-(\alpha t/m)}), \quad (6)$$

where  $p(t)$  represents the specific activity of the pool at any time  $t$  (Salser et al., 1968) Eq. 6 can be seen to be satisfactory for several conditions: (a) if the cells are growing in nonradioactive medium,  $A = 0$ , and therefore the pool specific activity  $p(t) = 0$ ; (b) at  $t = 0$ ,  $e^{-\alpha t/m} = 1$ , and  $p(t) = A(1 - 1) = 0$ ; and (c) as  $t \rightarrow \infty$ ,  $e^{-\alpha t/m} \rightarrow 0$ , and  $p(t) \rightarrow A$ .  $p(t)$  will approach  $A$  asymptotically with time and can never be greater than the specific activity of the starting material  $A$ .

The rate at which  $p(t)$  approaches  $A$  is dependent on the constant  $\alpha/m$ , the fractional turnover rate of the pool, which has the dimensions  $t^{-1}$ . Fig. 1 shows the different rates of approach to maximal specific activity with  $\alpha/m$  values ranging from 1.000 to 0.005. The lower the fractional turnover rate, the longer the time required to reach the maximal specific activity  $A$ .

The fractional turnover rate can be determined by making use of the relation  $\alpha t/m = -\ln [1 - p(t)]$ , which is directly derivable from Eq. 7 providing that the numerical constant  $A$  is placed equal to 1 (i.e., so that the maximal attainable specific activity is 100%). The slope of the line which results from plotting  $-\ln [1 - p(t)]$  on the  $y$ -axis against time  $t$  (in minutes) is equivalent to  $\alpha/m$  (in  $\text{minutes}^{-1}$ ).

#### *Kinetics of Uptake of Radioactivity into DNA*

DNA polymerases will incorporate into DNA molecules from this precursor pool whose specific activity  $p(t)$  is defined by Eq. 6; we assume that there is no compartmentation in the pool and that all molecules in the pool, whether labeled or unlabeled, have an equivalent probability of being incorporated into DNA at any time. We also assume that none of the DNA is degraded, or at least that the rate of degradation is negligible in comparison to the rate of synthesis. At time  $= 0$ , the specific activity of the pool  $p(t) = 0$  and no label enters the DNA; as time  $\rightarrow \infty$ ,  $p(t) = A$  and the rate of incorporation of label into DNA becomes the same as that of the rate of population growth, described by Eq. 1. If we define the amount of radioactivity in DNA at any time as  $y$ , then  $dy/dt$ , the rate of incorporation of label into DNA per unit volume, can be described in the following manner (Hanawalt, 1958):

$$\begin{aligned} \frac{dy}{dt} &= \frac{dN}{dt} \cdot p(t) \\ &= \frac{d(N_0 e^{\nu t})}{dt} \cdot A(1 - e^{-\alpha t/m}) \\ &= \nu N_0 e^{\nu t} A(1 - e^{-\alpha t/m}). \end{aligned} \quad (7)$$

Therefore,

$$\begin{aligned} y &= \int_0^t dy = \nu N_0 A \left( \int_0^t e^{\nu t} dt - \int_0^t e^{(\nu - \alpha/m)t} dt \right) \\ &= \nu N_0 A \{ [1/\nu] [e^{\nu t} - 1] - (1/[\nu - \alpha/m]) (e^{[\nu - \alpha/m]t} - 1) \} \\ &= \frac{N_0 A e^{\nu t}}{(\alpha/m) - \nu} ([\alpha/m][1 - e^{-\nu t}] - \nu[1 - e^{-\alpha t/m}]). \end{aligned} \quad (8)$$

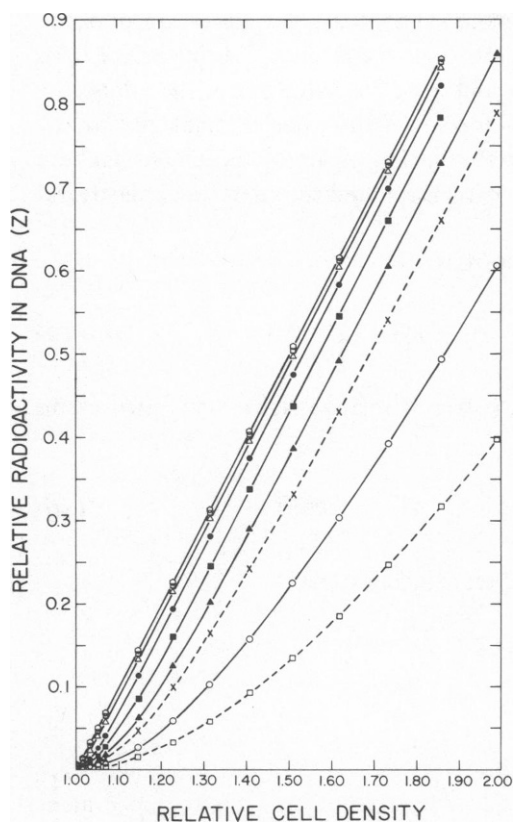


FIGURE 2

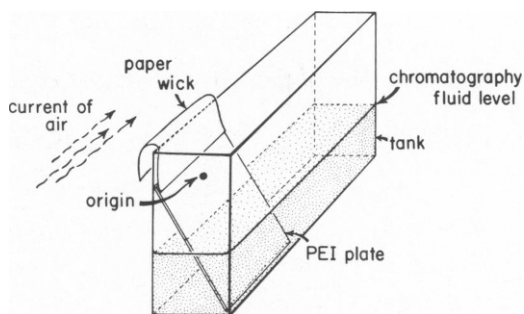


FIGURE 3

FIGURE 2 Theoretical accumulation of radioactivity into DNA with increasing cell density. The different curves are the results obtained from different values of  $\alpha/m$  for the direct precursor. Symbols and conditions are the same as for Fig. 1. Note that the symbols in Fig. 1 and 2 do not represent discrete data points and are included only for identification of the different curves.

FIGURE 3 Sketch of the chromatography apparatus showing wick draped outside the tank in a current of air. The top of the tank is put in place and weighted down with lead blocks.

Fig. 2 shows the dependence of  $y$  on the different fractional turnover rates of the precursor pool. A few general remarks should be made about  $y$ : (a) at  $t = 0$ ,  $1 - e^{-\nu t} = 0$ ,  $1 - e^{-\alpha t/m} = 0$ , and therefore  $y = 0$ ; (b) as  $t \rightarrow \infty$ , the equation simplifies to  $y = N_0 A e^{\nu t}$ , which will have the same slope as the growth curve of the cells; in other words, a plot of  $y$  vs. relative cell mass (omitting the constants  $N_0$  and  $A$ ) will approach unity regardless of the values of  $\nu$  or  $\alpha/m$ , the fractional turnover rate of the precursor pool.

#### *Relationship of the Kinetics of Accumulation of Labeled Molecules in the Precursor Pool to the Accumulation of Radioactivity in DNA*

In this section we shall relate the kinetics of incorporation of radioactivity into the candidate precursor pool and into DNA. As described in Kinetics of Uptake of Radioactivity into DNA above, a plot of  $y$  (Eq. 8) against relative cell mass, omitting the constants  $N_0$  and  $A$ , will approach as a limit a straight line with slope of unity. This straight portion of the curve is

easily determined from experimental data (see Results). The location of the intercept of this line on the  $x$ -axis is dependent on the growth constant,  $\nu$ , and the fractional turnover rate  $\alpha/m$ ; we will show that, over a wide range of values for  $\nu$  and  $\alpha/m$ , this value of  $x$  at the  $x$ -intercept corresponds to the time at which the precursor pool is 63–71% saturated. To show this we will first find the equation of the line approximating the linear portion of the DNA synthesis curve, use this equation to find the location of the  $x$ -intercept, and then determine the degree of pool saturation at that value of  $x$ .

Eq. 8, rewritten by omitting the constants  $N_0$  and  $A$ , is:

$$y = \frac{e^{\nu t}}{(\alpha/m) - \nu} \{ [\alpha/m][1 - e^{-\nu t}] - \nu[1 - e^{-\alpha t/m}] \}. \quad (9)$$

By substituting  $e^{\nu t} = x$  (or  $t = (\ln x)/\nu$ ), which is true if relative cell mass is used as the  $x$ -coordinate, Eq. 9 becomes

$$y = \frac{1}{(\alpha/m) - \nu} \{ \alpha x/m - \alpha m - \nu x + \nu x^{(1 - [\alpha/m\nu])} \}. \quad (10)$$

The derivative of this curve,  $dy/dx$ , after algebraic rearrangement is:

$$\frac{dy}{dx} = 1 - x^{-\alpha/m\nu},$$

so that

$$(1 - dy/dx)^{-m\nu/\alpha} = x. \quad (11)$$

The coordinate of any point  $(x_a, y_a)$  on this curve can be determined by substitution of this equality for  $x$  back into Eq. 10.

$$y_a = \frac{1}{(\alpha/m) - \nu} \{ ([\alpha/m] - \nu dy/dx)[1 - dy/dx]^{-m\nu/\alpha} - \alpha/m \} \quad (12)$$

Knowledge of the coordinates of the point  $(x_a, y_a)$  and of the slope of the asymptote of the curve ( $dy/dx$ ) at that point is sufficient to determine the intercept of the asymptote on the  $x$ -axis. By rearrangement of the general equation of the line  $y = (dy/dx)x + b$ , the  $x$ -intercept,  $(-b)(dy/dx)^{-1}$ , is

$$x_{\text{int}} = \frac{-b}{dy/dx} = x - \frac{y}{dy/dx}.$$

Again, after suitable substitution and rearrangement,

$$x_{\text{int}} = \frac{\alpha/m}{(dy/dx)([\alpha/m] - \nu)} (1 - [1 - dy/dx]^{[1 - m\nu/\alpha]}). \quad (13)$$

If the simplifying assumption that  $dy/dx = 1$  (which is only true for the asymptote as a limit, but is approximately true at large values of  $x$ ) is made, Eq. 13 reduces to:

$$x_{\text{int}} = \frac{\alpha/m}{(\alpha/m) - \nu}. \quad (14)$$

Eq. 6, the curve defining the specific activity of the pool  $p(t)$  at any time  $t$ , can be rewritten in terms of  $x$  by making use of the equality  $(\ln x)/\nu = t$  (and, again, by omitting the constant  $A$ ).

$$p(x) = 1 - x^{-\alpha/m\nu} \quad (15)$$

The specific activity at  $x_{\text{int}}$  ( $p[x_{\text{int}}]$ ), assuming that the slope of the asymptote  $dy/dx = 1$ , is therefore

$$p(x_{\text{int}}) = 1 - \{(\alpha/m)/[(\alpha/m) - \nu]\}^{-\alpha/m\nu}. \quad (16)$$

Representative values of  $p(x_{\text{int}})$  for different values of  $\alpha/m$  and  $\nu$  are presented in Table I. In our experiment, the approximate growth constant of the cells is  $\nu = 0.00344$ ; for a wide range of values of  $\alpha/m$ ,  $p(x_{\text{int}})$  remains within the range 0.63–0.71. Thus, the pool of the true precursor will be 63–71% saturated at the time corresponding to  $x_{\text{int}}$ ; this fact will be used in the analysis of our experimental data. It should also be noted that this relationship is true for a wide range of  $\nu$  values, so that little error is introduced by uncertainty in determining the cellular growth rate.

## MATERIALS AND METHODS

### *Bacteria and Growth Media*

*E. coli* K12 DG75 (W1485 F<sup>-</sup> thy A leu deoC/deoB) and K12 W3110 were used. Growth media were constructed from the following solutions: (a) Tris buffer and salts, hereafter referred to as "Tris medium," containing  $4.5 \times 10^{-2}$  M inorganic phosphate (Hanawalt and Cooper, 1971); (b) "Tris minus phosphate" was Tris medium without added phosphate; (c) "solution A minus phosphate" was a 10-fold concentrate of "Tris minus phosphate" (without MgCl<sub>2</sub>) adjusted to pH 7.5 before autoclaving; (d) "solution B" was a 100-fold concentrate of the MgCl<sub>2</sub> in Tris minus phosphate. When required, growth supplements were 0.2% glucose, 20  $\mu$ g leucine per ml, and 3  $\mu$ g thymine per ml.

Preconditioned growth medium was made by inoculating low phosphate Tris medium (containing  $1.4 \times 10^{-3}$  M inorganic phosphate) plus 0.2% glucose with W3110 and allowing the culture to reach stationary phase. The medium was passed through several Millipore 0.45- $\mu$ m, pore-size nitrocellulose filters (Millipore Corp., Bedford, Mass.), at least once through a 0.22- $\mu$ m, pore-size filter, and filtered sterilely through a 0.22- $\mu$ m, pore-size filter. The filtrate had a lower pH (4.8 instead of 7.3) and had been depleted in one or more of the components of the original medium by the bacterial growth. Constituents of the original medium were returned in the following manner. 24.9 ml W3110 pregrown medium, 1.2 ml Tris medium, 3.0 ml solution A minus phosphate, and 0.3 ml each of 20% glucose, 2 mg/ml leucine, and 0.3 mg/ml thymine were mixed together and let stand for 10 min. Then 0.03 ml solution B was added. The resulting medium (called "W3110 pg plus thymine") was buffered at pH

TABLE I  
VALUES OF  $p(x_{\text{int}})$  AS A FUNCTION OF  $\alpha/m$  AND  $\nu$

$\nu$	$\alpha/m$							
	1.0	0.5	0.25	0.10	0.05	0.02	0.01	0.005
0.00115, $\tau = 603$ min	0.639	0.645	0.659	0.706	0.816	—	—	—
0.00344, $\tau = 201.5$ min	0.633	0.633	0.635	0.639	0.645	0.666	0.706	0.816
0.01032, $\tau = 67.2$ min	0.634	0.636	0.640	0.652	0.674	0.756	—	—

7.3–7.4 and supported bacterial growth at approximately the same growth rate but to a higher cell density than the nonpreconditioned medium.

### *Conditions for Isotopic Labeling*

DG75 was grown for several generations in W3110 pg plus thymine from a single colony at 25°C. When the cells were in mid-log phase they were diluted in the same medium containing 82  $\mu\text{Ci/ml}$   $\text{H}_3^{32}\text{PO}_4$  (in 0.02 N HCl, New England Nuclear Corp., Boston, Mass.) and allowed to grow for 3–4 generations before labeling with [ $^3\text{H}$ ]-thymine was begun.

[ $^3\text{H}$ ]-methyl-thymine (57.2 Ci/mmol, in ethanol: water 7:3; New England Nuclear Corp.) was evaporated to dryness on ice under nitrogen. An amount of W3110 pg (without thymine) containing approximately the same specific activity of  $^{32}\text{P}$  (84  $\mu\text{Ci/ml}$ ) as the growth medium above was added so that the total thymine concentration was that of the growth medium (3  $\mu\text{g/ml}$ ).

Autoradiography was performed by wrapping the polyethyleneimine (PEI) plate in Saran Wrap (Dow Chemical, Indianapolis, Ind.) and placing it adjacent to a sheet of Kodak RPR or XR-1 x-ray film (Eastman Kodak Co., Rochester, N.Y.) in the dark for 24–48 h.

### *Sample Preparation for Assay of Radioactivity in DNA and Soluble Nucleotide Pools*

200- $\mu\text{l}$  samples of the culture were removed and added to 40  $\mu\text{l}$  ice-cold 2.4 M  $\text{HClO}_4$ . Two 50- $\mu\text{l}$  samples were withdrawn as soon as possible for assay of radioactivity in DNA as described below. The remaining 140  $\mu\text{l}$  were allowed to stand on ice for 80–140 min before centrifugation in 0.4 ml capacity plastic microcentrifuge tubes for 15 min at 8,000 rpm. To 100  $\mu\text{l}$  of the supernatant 10  $\mu\text{l}$  2.88 M KOH, 0.64 M  $\text{KHCO}_3$  was added. The white  $\text{KCLO}_4$  precipitate was allowed to stand on ice for at least 15 min before removal by centrifugation for 15 min at 8,000 rpm. The supernates ("final cell extracts") were at approximately neutral pH and were stored at  $-10^\circ\text{C}$ . This method is a modification of that of Bagnara and Finch (1972).

5  $\mu\text{l}$  of each of the 50  $\mu\text{l}$  0.4 M  $\text{HClO}_4$  samples was removed and placed in a shell vial for assay of total radioactivity by liquid scintillation counting in 3 ml Insta-Gel (Packard Instrument Co., Inc., Downers Grove, Ill.). 5  $\mu\text{g}$  unlabeled DNA and 75  $\mu\text{l}$  6 N NaOH were added to the remaining 45  $\mu\text{l}$ , and the mixture was incubated for 4.5 h at  $37^\circ\text{C}$  to thoroughly hydrolyze RNA. The samples were reacidified with 75  $\mu\text{l}$  ice-cold 8 N HCl, and 4 ml 10% trichloroacetic acid (TCA) containing 1 mg/ml thymine was then added. The mixture was filtered through a 25 mm diameter 0.45  $\mu\text{m}$  pore size Millipore nitrocellulose filter presoaked in 2 mg/ml thymine. The tube was rinsed three times with 3 ml 10% TCA plus 1 mg/ml thymine, and the filter was rinsed twice with 95% ethanol and twice with glass distilled water. The filters were dried and assayed for radioactivity by liquid scintillation counting in Omnifluor (New England Nuclear Corp.).

### *Chromatographic Procedures*

**dTTP** Yegian (1974) outlined a procedure for the one-dimensional, thin-layer chromatography of the four deoxynucleoside triphosphates. A periodate oxidation step was performed before chromatography to remove ribonucleotides. Though in our hands the procedure worked quite well, the yield of nucleotide was somewhat variable and we had difficulty applying the periodate oxidized material to the thin-layer sheet. Our modified procedure, described below, is suitable only for dTTP but does not require the periodate oxidation step.

The final cell extract was mixed with unlabeled dTTP (usually 70  $\mu\text{l}$  of extract with  $4 \times 10^{-8}$  mol dTTP) and applied 5  $\mu\text{l}$  at a time, with intermediate drying, to a spot 4 cm from one edge of a 20  $\times$  2.5-cm Brinkmann polygram cel 300 PEI impregnated cellulose plastic sheet (Brinkmann Instruments, Inc., Westburg, N.Y.). (The sheets were first washed in the following way: A 20  $\times$  20-cm PEI plate was first laid face down in a solution of 10% NaCl for 10–20 min; care was taken to avoid bubble formation between the plate and the liquid. The plate was then left to dry in air for a few hours before being laid face down in glass distilled water for 10 min. When dry, the plate was laid down in pH 2.2 pyridine formate (2 M formic acid adjusted to pH 2.2 with pyridine) for 10 min, air dried briefly, and laid down



once more in glass distilled water for 10 min. Once dry, the plates were stacked on top of each other, layer against layer, wrapped in aluminum foil, and stored in darkness at  $-20^{\circ}\text{C}$ . We are indebted to Dr. D. Brutlag for informing us of this procedure which is a modification of previously published procedures (Randerath and Randerath, 1967; Southern and Mitchell, 1971). After application of the entire sample the plate was placed face up in 95% ethanol for 15 min. A  $15 \times 2.5\text{-cm}$  wick of Whatman 3-mm paper (Whatman, Inc., Clifton, N.J.) was stapled to the end closest to the origin, and plate and wick were thoroughly sprayed with glass distilled water. The plate was then immersed to a depth of  $\sim 12\text{ cm}$  in 2 M formic acid-0.5 M LiCl. The chromatography tank was covered, with one end of the wick draped outside the tank in a current of cool air created by a fan (see Fig. 3). Development for 2 h resulted in the movement of bases, nucleosides, monophosphates, diphosphates, diphospho-sugars, and some triphosphates well off the origin. The plate was dried and cut  $\sim 0.5\text{ cm}$  ahead of the dTTP spot which was visualized under germicidal UV light. We then immersed the plate face up in Tris-methanol (600 mg Trizma base [Sigma Chemical Co., St. Louis, Mo.] in 500 ml methanol) (Randerath and Randerath,

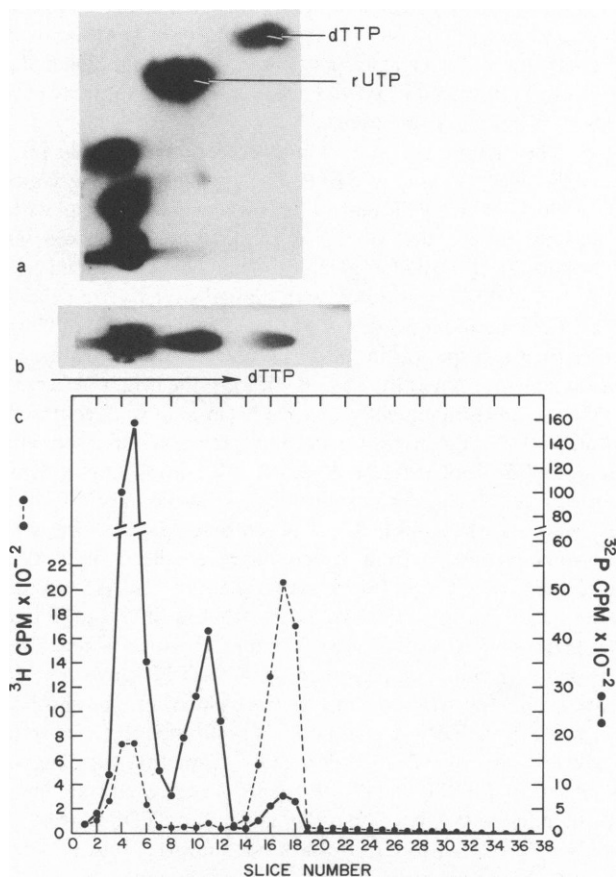


FIGURE 4 Chromatography of dTTP. (a) Autoradiogram of an extract chromatographed on a  $20 \times 20\text{-cm}$  sheet as described in the text, and then subjected to development in  $0.45\text{ M }(\text{NH}_4)_2\text{SO}_4$  pH 8.0 (Yegian, 1974) perpendicular to both directions. (The first direction of chromatography is to the left, second direction is towards the right, and third is vertically upwards.) Note that dTTP migrates as a single spot, and that rUTP carries a small impurity that was resolved by the  $(\text{NH}_4)_2\text{SO}_4$ . (b) Autoradiogram of a typical sample of dTTP chromatography. The same extract used in a was chromatographed in the same way but without the third  $(\text{NH}_4)_2\text{SO}_4$  development. (c) After autoradiography, the plate was assayed for radioactivity as described in Methods.

1967) for 5 min, dried it in a current of warm air, immersed it in 95% ethanol for 15 min, and dried it again. A 5-cm-long wick was then stapled to the end farthest from the origin and, this time without previous spraying with water, the plate was placed origin-end down to a depth of 0.3 cm in a solution of 23.12 g ammonium acetate, 7.5 g boric acid, and 100 ml H<sub>2</sub>O for ~4 h. dTTP migrates 6–10 cm from the origin and is clearly resolved from ribouridine triphosphate. The entire plate was sliced into several 0.5-cm-wide pieces cut perpendicularly to the direction(s) of chromatography (Fig. 4), and each slice assayed for radioactivity by immersing the strip for 15 min in 1 ml 0.7 M MgCl<sub>2</sub>:Tris-hydrochloride pH 7.4 (100:2), then adding 10 ml Triton X-100 (Rohm and Hans Co., Philadelphia, Pa.):Omnifluor (1:2), and agitating thoroughly. A typical result is shown in Fig. 4.

We believe that the dTTP obtained in this procedure is highly (>95%) pure for the following reasons: (a) the <sup>3</sup>H:<sup>32</sup>P ratio from the one-dimensional procedure is higher than that obtained from any two-dimensional procedure that we have tried (Randerath and Randerath, 1967), indicating greater contamination in the latter from other <sup>32</sup>P-containing compounds (data not shown); (b) the <sup>3</sup>H:<sup>32</sup>P ratio is relatively constant over the entire peak (Fig. 4c), indicating high purity; and (c) if the above procedure is followed on one side of a 20 × 20-cm sheet, and the sheet is developed a third time perpendicular to the direction(s) of chromatography with a solvent that chiefly resolves compounds by the basis of its base moiety, the dTTP chromatographs as a single spot (Fig. 4a). It should be noted that none of the above procedures is capable of distinguishing dTTP from deoxyuridine triphosphate (dUTP). We do not know the intracellular level of dUTP in the strain used.

**dTDP-SUGARS** The one-dimensional, thin-layer chromatographic procedure for the dTDP-sugars is similar in general concept to that of dTTP. The application of the sample to a spot 4 cm from the edge of a 20 × 4-cm, washed PEI plate and subsequent washing with 95% ethanol before chromatography is identical except that 60 μl of cell extract are mixed with  $8 \times 10^{-8}$  mol of deoxythymidine diphosphate glucose (dTDP-glucose). The wick is attached to the side closest to the origin. After both wick and plate are saturated with glass-distilled water, the plate is immersed to a depth of ~12 cm in 0.1 M ammonium acetate-4 M acetic acid for 2–3 h. The dTDP-glucose marker migrates as a ring rather than as a spot (as in the dTTP procedure); the plate is cut 0.5 cm ahead of the most forward point of the marker, generally 2.0–3.0 cm from the origin. After the plate is washed with Tris-methanol, 95% ethanol, and subsequently dried, a 5-cm-long wick is attached to the end farthest from the origin. The end closest to the origin is placed in a solution of 6 g sodium borate (Na<sub>2</sub>B<sub>4</sub>O<sub>7</sub> · 10 H<sub>2</sub>O), 10.5 g boric acid, and 62.5 ml ethylene glycol in 177.5 ml H<sub>2</sub>O to a depth of ~0.3 cm. A wick change is usually required after 10 h of chromatography (when the solvent front has proceeded through more than half the length of the wick); 13 h of chromatography are sufficient to resolve the dTDP-glucose spot from a secondary front which migrates ahead of it and the bulk of the <sup>32</sup>P radioactivity behind it (Fig. 5). The dTDP-glucose marker always had the same form as the autoradiographic profile shown in Fig. 5; thus, we believe that most of the <sup>32</sup>P in the area indicated is in fact dTDP-sugar. The plate is sliced and assayed for radioactivity as before. The total radioactivity is greater in the dTDP-sugar chromatography than in the dTTP procedure in part because many diphosphates, diphosphosugars and triphosphates that are eluted off the sheet in the dTTP procedure remain near the origin when the dTDP-sugar isolation is performed. If the chromatogram is made from a culture labeled for several generations with <sup>32</sup>PO<sub>4</sub> and [<sup>3</sup>H]-methyl thymine, and the specific activity (measured as the <sup>3</sup>H:<sup>32</sup>P ratio) of dTTP and dTDP-sugars is compared (making allowances for the fact that the molar ratio of thymine to PO<sub>4</sub> is 1:3 in dTTP and 1:2 in dTDP-glucose), the specific activity of the dTDP sugars is only 69% of that of dTTP (data not shown). Thus, ~30% of the <sup>32</sup>P label in the dTDP-glucose region does not contain a radioactively labeled thymine moiety.

## RESULTS AND DISCUSSION

A bacterial population in a state of balanced exponential growth will incorporate [<sup>3</sup>H]-thymine into DNA in the manner described by Eq. 8. When plotted against relative cell mass (optical density at 450 nm [OD<sub>450</sub>]) the increase in radioactivity becomes linear, with an *x*-intercept defined by Eq. 14. The *x*-intercept is easily determined by regression analysis from

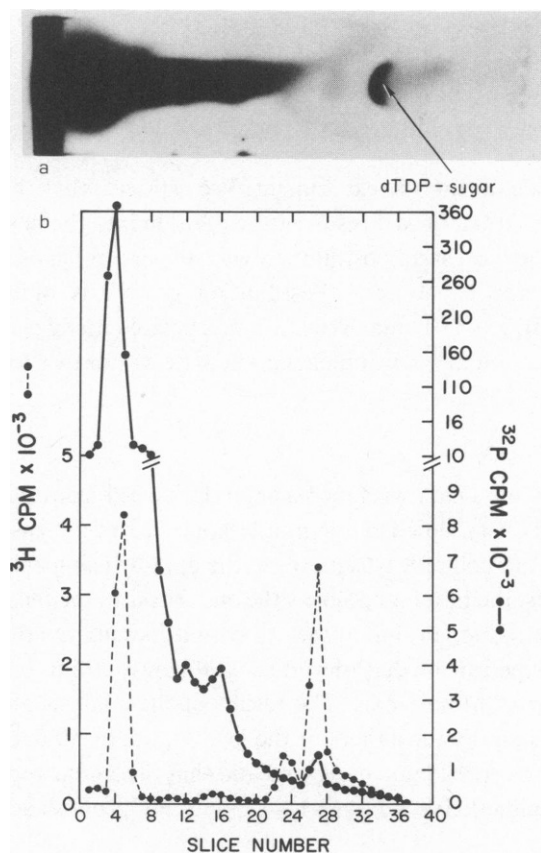


FIGURE 5

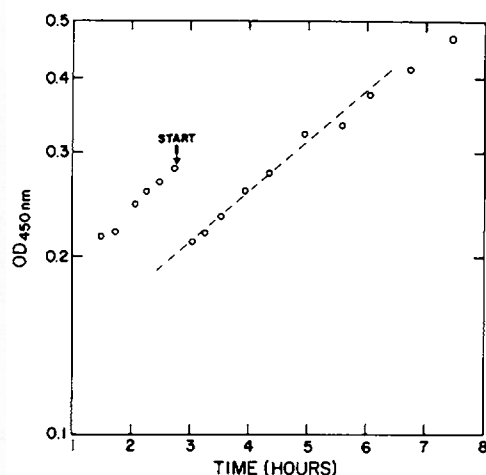


FIGURE 6

FIGURE 5 dTDP-sugar chromatography. Chromatography was performed as described in Methods. (a) Autoradiogram. (b) Radioactivity assay. Scaling factor not used for correspondence with autoradiogram. FIGURE 6 Optical density of  $^{32}\text{P}$ -labeled *E. coli* DG75 before and during the  $^3\text{H}$ thymine "pulse." The straight line represents growth with a doubling time of 201.33 min. "Start" indicates the time of dilution into medium containing  $^3\text{H}$ thymine and  $^{32}\text{P}$ .

the incorporation data. The intracellular pool of the immediate precursor of DNA-thymine should be at 63–71% of its maximal specific activity at the optical density corresponding to the x-intercept of the DNA incorporation data (see Theoretical). To study the kinetics of thymine incorporation into nucleotide pools and into DNA, the following experimental protocol was devised: (a) The bacterial culture was prelabeled for several generations with  $\text{H}_3^{32}\text{PO}_4$  to uniformly label the nucleotide pools; and (b) the  $^3\text{H}$ thymine labeling was started by diluting the culture into fresh medium containing  $\text{H}_3^{32}\text{PO}_4$  and  $^3\text{H}$ thymine such that the  $^{32}\text{P}$  specific activity and the thymine concentration were not altered by the labeling conditions.

*E. coli* K12 DG75 was grown from a single colony for several generations in low-phosphate, preconditioned medium at 25°C. The doubling time of the culture was ~190 min. While in exponential growth the cells were diluted ~100-fold into medium containing a final concentration of 82  $\mu\text{Ci/ml}$   $\text{H}_3^{32}\text{PO}_4$  and allowed to grow to an optical density at 450 nm of 0.28–0.29. The entire culture was then poured into a flask of prewarmed medium containing

$^{32}\text{P}$  and the same concentration of  $[^3\text{H}]$ thymine. Samples were removed over the course of almost one generation for optical density measurement and for the assay of radioactivity in soluble pools and DNA as described in Methods.

### *Cellular Growth*

Fig. 6 shows the optical density of the culture during the experiment. We estimate that the doubling time,  $\tau$ , increased from 190 min to  $\sim 200$  min as a result of the dilution into the new medium, but that the growth rate was relatively constant postdilution with the exception of a small decline in the growth rate late in the experiment. Postdilution growth is quite adequately represented by a straight line with  $\tau = 201$  min. We have interpolated along this line to estimate the optical density of the culture at each time a sample was withdrawn for analysis.

### *Kinetics of Uptake of $^3\text{H}$ -Label into DNA*

Fig. 7 shows the increase of  $^3\text{H}$ -radioactivity into DNA with increasing relative cell mass. As predicted, the rate of  $^3\text{H}$  uptake was initially very slow but eventually appeared to increase linearly with cell mass. We have applied the method of least squares to the data by using only the last 10, 20, 30, 40, 50, or all 60 data points; the best regression is the one that uses the most data (thus reducing the error variance; see Introduction) but at the same time does not use the data points from the beginning of the experiment that deviate significantly from the extrapolation of the linear portion of the curve to the x-axis. The results of the analysis are shown in Table II. The regression line is essentially unchanged if the last 30, 40, or 50 data points are used; we conclude that the data fit our prediction quite well and that the x-intercept of the linear region of the data lies in the region 0.206–0.210  $\text{OD}_{450}$  U (with 95% confidence limits of 0.201–0.215  $\text{OD}_{450}$  U).

### *Kinetics of Uptake of Radioactivity into Acid-Soluble Pools*

Fig. 8 displays the change in the specific activity of dTTP and dTDP-sugars during the course of the experiment. As would be predicted by their relative positions in the biochemical pathway, the uptake of radioactivity into dTTP is much more rapid than it is for dTDP-sugars. The shape of the dTTP curve seems to indicate that it has reached its maximal specific

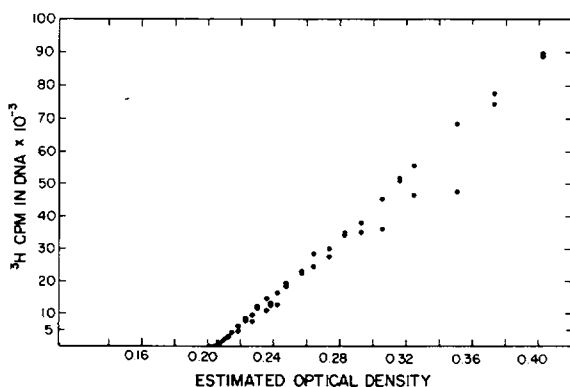


FIGURE 7 Increase of  $^3\text{H}$ -radioactivity in DNA with increasing cell mass.

TABLE II  
REGRESSION ANALYSIS OF DNA SYNTHESIS DATA

N	Slope	Correlation coefficient	x-Intercept	95% Confidence limits	
				Slope	x-Intercept
60	$4.36 \times 10^5$	0.993	0.205	$\pm 1.38 \times 10^4$	0.203–0.207
50	$4.40 \times 10^5$	0.991	0.206	$\pm 1.64 \times 10^4$	0.203–0.209
40	$4.42 \times 10^5$	0.989	0.207	$\pm 2.11 \times 10^4$	0.202–0.211
30	$4.47 \times 10^5$	0.984	0.208	$\pm 3.10 \times 10^4$	0.201–0.215
20	$4.52 \times 10^5$	0.971	0.210	$\pm 5.51 \times 10^4$	0.193–0.222
10	$4.64 \times 10^5$	0.924	0.213	$\pm 1.51 \times 10^5$	0.145–0.249

N, Number of points used for analysis.

activity by the conclusion of the experiment, while the specific activity of the dTDP-sugar pool is still increasing. However, when the different molar ratio of phosphate to thymine and the 30% impurity in the dTDP-sugar chromatography (see Methods) are taken into account, it is found that the dTDP-sugar pool is at least very near its maximal specific activity as well.

As shown in Fig. 8, the OD (450 nm) at which dTTP was 63% saturated was  $\sim 0.208$ , well within the range established for the x-intercept from the DNA synthesis data. The OD range for which the dTDP-sugar pool is 63–71% saturated (assuming that the final value represents 100%) is  $\sim 0.26$ , far removed from that of the x-intercept. Thus, we conclude that the labeling kinetics are consistent with the hypothesis that dTTP is the direct precursor of thymine in DNA, and we believe that we can rule out the possibility that DNA polymerases use one (or more) dTDP-sugar for DNA replication. We hasten to add, however, that an experiment of this type cannot prove that dTTP is the precursor, but can only provide evidence that confirms (or fails to confirm) this hypothesis. In particular, this experimental design cannot distinguish

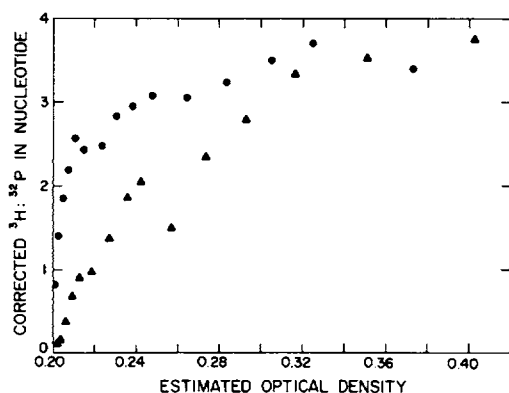


FIGURE 8

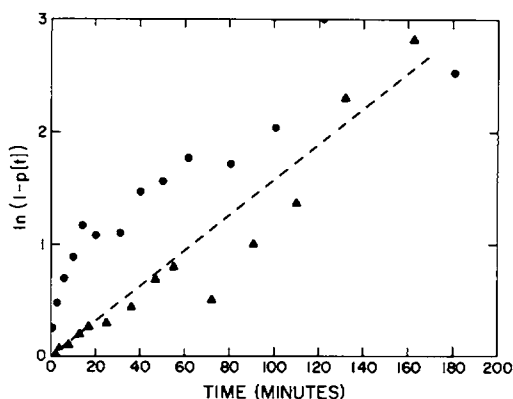


FIGURE 9

FIGURE 8 Change in the specific activity of dTTP and dTDP-sugars with increasing cell mass. The  $^3\text{H}:^{32}\text{P}$  ratio was determined from the chromatograms as described in Methods. A correction was made for  $^{32}\text{P}$  decay during the sample counting in the scintillation counter. dTTP,  $\bullet$ - $\bullet$ ; dTDP-sugars,  $\blacktriangle$ - $\blacktriangle$ .

FIGURE 9 Determination of the fractional turnover rate of the intracellular pools from the data displayed in Fig. 8. The slope of the curve gives the value of  $\alpha/m$  in  $\text{min}^{-1}$  (see Theoretical). dTTP,  $\bullet$ - $\bullet$ ; dTDP-sugars,  $\blacktriangle$ - $\blacktriangle$ .

between nucleotide pools that equilibrate rapidly with one another, and therefore cannot distinguish dTTP from dTDP or dTMP.

Our conclusions depend very heavily on our ability to measure the specific activity of the pools available to DNA polymerases accurately. If, for instance, there was physical or chemical compartmentation of the intracellular pools destroyed by our lysis procedure, our pool measurements would not truly represent the pool that was used for DNA synthesis. Although compartmentation of nucleotide pools has been reported in eukaryotic systems (Wiegers et al., 1976), we know of no evidence for this in bacteria. Another problem lies in the deviation in the curvature of the dTTP labeling curve from that predicted. Fig. 9 shows that although an approximate value of  $\alpha/m = 0.015 \text{ min}^{-1}$  can be estimated for the dTDP-sugar pool, no such estimate can be made for dTTP. The pool specific activity appears either to increase more rapidly at first or more slowly later on than we anticipated. There exist at least two possibilities for this discrepancy. Hosono et al. (1975) have reported transient increases in the size of the dTTP pool resulting from a deoxythymidine impurity in their [ $^3\text{H}$ ]thymine. Although the effects that they observed were much more striking than ours, and although we could detect no [ $^3\text{H}$ ]deoxythymidine in our [ $^3\text{H}$ ]thymine chromatographically (data not shown), it remains possible that a very minor impurity, too small for us to detect, was responsible for the high rate of labeling of the pool early in the experiment. Another possibility that we did not take into account in constructing our model is the effect of "recycling" of the deoxythymidine moiety of dTDP-sugars into the rest of the deoxythymidine nucleotide pools. Molecules derived from the low specific activity dTDP-sugar pool would effectively lower the input specific activity until the dTDP-sugar pool itself had reached its maximal specific activity. The net effect would be to make the fractional turnover rate of the dTTP pool appear to be smaller than it actually was. We favor this latter hypothesis, but more work will have to be done on the biological role and rate of turnover of dTDP-sugars in *E. coli* before this hypothesis can be tested. The role of the large deoxythymidine diphosphate sugar pool in the metabolism of *Escherichia coli* remains to be elucidated.

We wish to thank Priscilla Cooper, Ann Ganesan, and C. A. Smith for providing invaluable assistance and encouragement throughout the course of this study. We would also like to thank Mr. D. Fischer for help with the theoretical modeling, and Mr. B. Howe for computer programming and for making the Stanford Hydraulics Laboratory facility available for our use.

This work was supported by a grant, GM09901-17, from the National Institute of General Medical Sciences.

Received for publication 28 February 1978 and in revised form 14 June 1979.

## REFERENCES

- BAGNARA, A. S., and L. R. FINCH. 1972. Quantitative extraction and estimation of intracellular nucleoside triphosphates of *Escherichia coli*. *Anal. Biochem.* 45:24-34.
- COOPER, H. L. 1973. Analysis of precursor pool labeling kinetics without pool size measurements: a computer-assisted approach. *Anal. Biochem.* 53:49-63.
- GEFTER, M. L., Y. HIROTA, T. KORNBERG, J. A. WECHSLER, and C. BARNOUX. 1971. Analysis of DNA polymerases II and III in mutants of *Escherichia coli* thermosensitive for DNA synthesis. *Proc. Natl. Acad. Sci. U.S.A.* 68:3150-3153.
- GOLDSTEIN, A. 1964. *Biostatistics: An Introductory Text*. Macmillan Co., New York.
- HANAWALT, P. C. 1958. Macromolecular synthesis in *Escherichia coli* during conditions of unbalanced growth. Ph.D. thesis, Yale University, New Haven, Conn. University Microfilms, Ann Arbor, Mich.
- HANAWALT, P. C., and P. K. COOPER. 1971. Determination of repair replication *in vivo*. *Methods Enzymol.* 21:221-230.

- HOSONO, R., H. HOSONO, and S. KUNO. 1975. Effects of growth conditions on thymidine nucleotide pools in *E. coli*. *J. Biochem. (Tokyo)* **78**:123-129.
- KAHN, M. 1976. Intermediates in bacteriophage P4 DNA replication. Ph.D. thesis, Stanford University, Stanford, Calif. University Microfilms, Ann Arbor, Mich.
- KORNBERG, A. 1974. *DNA Synthesis*. W. H. Freeman and Co. Publishers, San Francisco. 399 pp.
- KORNBERG, T. 1975. Studies on the *in vitro* replication of the *Escherichia coli* chromosome. In *DNA Synthesis and its Regulation*. M. Goulian, P. Hanawalt, and C. F. Fox, editors. W. A. Benjamin, Inc., Menlo Park, Calif. 296-302.
- KORNBERG, T., A. LOCKWOOD, and A. WORCEL. 1974. Replication of the *Escherichia coli* chromosome with a soluble enzyme system. *Proc. Natl. Acad. Sci. U.S.A.* **71**:3189-3193.
- MASKER, W. E., and P. C. HANAWALT. 1973. Ultraviolet-stimulated DNA synthesis in toluenized *Escherichia coli* deficient in DNA polymerase I. *Proc. Natl. Acad. Sci. U.S.A.* **70**:129-133.
- MOSES, R. E. and C. C. RICHARDSON. 1970. Replication and repair of DNA in cells of *Escherichia coli* treated with toluene. *Proc. Natl. Acad. Sci. U.S.A.* **67**:674-681.
- NÜSSLEIN, V., B. OTTO, F. BONHOEFFER, and H. SCHALLER. 1971. Function of DNA Polymerase III in DNA Replication. *Nat. New Biol.* **234**:285-286.
- OHKAWA, T. 1976. Studies of intracellular thymidine nucleotides: relationship between the synthesis of deoxyribonucleic acid and the thymidine triphosphate pool in *Escherichia coli* K12. *Eur. J. Biochem.* **61**:81-91.
- OKAZAKI, R., T. OKAZAKI, and Y. KURIKI. 1960. Isolation of thymidine diphosphate rhamnose and a novel thymidine diphosphate sugar compound from *Escherichia coli* strain B. *Biochim. Biophys. Acta.* **38**:384-386.
- OKAZAKI, T., J. L. STROMINGER, and R. OKAZAKI. 1963. Thymidine diphosphate-L-rhamnose metabolism in smooth and rough strains of *Escherichia coli* and *Salmonella weslaco*. *J. Bacteriol.* **86**:118-124.
- POWELL, E. O. 1956. Growth rate and generation time of bacteria, with special reference to continuous culture. *J. Gen. Microbiol.* **15**:492-511.
- RANDERATH, K., and E. RANDERATH. 1967. Thin-layer separation methods for nucleic acid derivatives. *Methods Enzymol.* **12A**:323-347.
- RUBINOW, S. I., and A. YEN. 1972. Quantitation of some DNA precursor data. *Nat. New Biol.* **239**:73-74.
- SALSER, W., J. JANIN, and C. LEVINthal. 1968. Measurement of the unstable RNA in exponentially growing cultures of *Bacillus subtilis* and *Escherichia coli*. *J. Mol. Biol.* **31**:237-266.
- SOUTHERN, E. M., and A. R. MITCHELL. 1971. Chromatography of nucleic acid digests on thin layers of cellulose impregnated with polyethyleneimine. *Biochem. J.* **123**:613-617.
- WERNER, R. 1971. Mechanism of DNA replication. *Nature (Lond.)* **230**:570-572.
- WIEGERS, U., G. KRAMER, K. KLAPPROTH, and H. HILZ. 1976. Separate pyrimidine-nucleotide pools for messenger-RNA and ribosomal-RNA synthesis in HeLa S3 cells. *Eur. J. Biochem.* **64**:535-540.
- YEGIAN, C. D. 1974. A procedure for the measurement of intracellular deoxyribonucleoside triphosphate pools by thin layer chromatography. *Anal. Biochem.* **58**:231-237.